Breast Cancer RESEARCH

RESEARCH ARTICLE Open Access

HER3 and downstream pathways are involved in colonization of brain metastases from breast cancer

Leonard Da Silva[1,2,3], Peter T Simpson[1,2], Chanel E Smart[1,2], Sibylle Cocciardi[2], Nic Waddell[2], Annette Lane[1], Brian J Morrison[2,4], Ana Cristina Vargas[1], Sue Healey[2], Jonathan Beesley[2], Pria Pakkiri[1], Suzanne Parry[1,2], Nyoman Kurniawan[5], Lynne Reid[1,2], Patricia Keith[1,2], Paulo Faria[7,6], Emilio Pereira[8], Alena Skalova[9], Michael Bilous[10], Rosemary L Balleine[11], Hongdo Do[12], Alexander Dobrovic[12], Stephen Fox[12], Marcello Franco[3], Brent Reynolds[13,16], Kum Kum Khanna[14], Margaret Cummings[1,14], Georgia Chenevix-Trench[2], Sunil R Lakhani[1,2,15*]

Abstract

Introduction: Metastases to the brain from breast cancer have a high mortality, and basal-like breast cancers have a propensity for brain metastases. However, the mechanisms that allow cells to colonize the brain are unclear.

Methods: We used morphology, immunohistochemistry, gene expression and somatic mutation profiling to analyze 39 matched pairs of primary breast cancers and brain metastases, 22 unmatched brain metastases of breast cancer, 11 non-breast brain metastases and 6 autopsy cases of patients with breast cancer metastases to multiple sites, including the brain.

Results: Most brain metastases were triple negative and *basal-like*. The brain metastases over-expressed one or more members of the HER family and in particular HER3 was significantly over-expressed relative to matched primary tumors. Brain metastases from breast and other primary sites, and metastases to multiple organs in the autopsied cases, also contained somatic mutations in *EGFR, HRAS, KRAS*, *NRAS* or *PIK3CA*. This paralleled the frequent activation of AKT and MAPK pathways. In particular, activation of the MAPK pathway was increased in the brain metastases compared to the primary tumors.

Conclusions: Deregulated HER family receptors, particularly HER3, and their downstream pathways are implicated in colonization of brain metastasis. The need for HER family receptors to dimerize for activation suggests that tumors may be susceptible to combinations of anti-HER family inhibitors, and may even be effective in the absence of *HER2* amplification (that is, in triple negative/basal cancers). However, the presence of activating mutations in *PIK3CA*, *HRAS, KRAS* and *NRAS* suggests the necessity for also specifically targeting downstream molecules.

Introduction

Among women with breast cancer, 30% to 40% will develop metastatic disease. The natural history of metastatic breast cancer to the brain is of symptomatic disease in 10% to 20% of these patients and a dismal mean survival of six months following diagnosis [1,2]. Associations with younger age, p53 positivity, estrogen receptor (ER) negative and epidermal growth factor receptor 1 (EGFR) and two (HER2) positive cancers have been reported [3-5]. The epidermal growth factor receptor family comprises four receptors, HER1 to 4. Upon activation, hetero or homo-dimerization occurs, followed by phosphorylation of specific tyrosine residues in the intracellular domain, stimulating signaling cascades mediated mainly by AKT and MAPK and the regulation of cell proliferation, angiogenesis, migration and survival [6,7].

* Correspondence: s.lakhani@uq.edu.au
[1]Molecular & Cellular Pathology, The University of Queensland Centre for Clinical Research, & School of Medicine, Building 918/B71, RBWH complex, Brisbane, 4029, Australia

Basal-like tumors are generally high grade, negative for ER, progesterone receptors (PgR) and HER2 (that is, *triple negative*) [8]. The current dogma would predict that these tumors are unlikely to respond to endocrine and trastuzumab-based therapy and no targeted therapy is currently available, although clinical trials are ongoing [8]. Despite being node negative, a proportion of patients subsequently present with distant metastases, particularly to the brain [9,10]

Using autopsy records of breast cancer patients, Paget [11] demonstrated a non-random pattern of metastatic spread. This suggested that tumor cells (the *seed*) could have a specific affinity for the microenvironment of certain organs (the *soil*). In agreement, animal models demonstrate that particular sets of genes can increase the potential of breast cancer cell lines to colonize specific distant sites, for example, bone, lung [12,13]; and brain [14,15].

The cancer *mutatome* is very complex, with more than 140 CAN genes identified which are mutated at a significant frequency in cancer [16,17]. The genomic landscape of breast cancer is also very complex and heterogeneous, with different subgroups of tumours (luminal, basal, HER2) harboring different types and patterns of mutations [18]. There is also evidence that breast cancer cell lines with a basal phenotype have a higher frequency of mutations in *BRAF, KRAS*, and *HRAS* than luminal breast cancer cell lines [19-21].

We have analyzed a relatively large and rare set of human tumors to elucidate the mechanisms involved in colonization of the brain. Samples studied involved matched pairs of primary breast cancer and brain metastases, unmatched brain metastases, non-breast brain metastases and autopsy cases of breast cancer patients with metastases to multiple sites, including the brain. We provide evidence of increased activation of HER3 and downstream pathway molecules in brain metastases from breast cancer and suggest that the inhibition of HER family receptors, even in the absence of *HER2* gene amplification (for example, triple negative/basal cancers), could play a significant role in the management of patients with brain metastases from breast cancer. In addition, we demonstrated the possible fallacies of this approach without considering the presence of somatic activating mutations in downstream molecules [22-24].

Materials and methods

Additional detailed methodologies (see Additional file 1). The study was approved by the local research ethics committees under the project number UQ2005000785 and RBHW 2005/22.

Clinical samples

All human clinical samples studied were available as formalin fixed-paraffin embedded (FFPE) tumor blocks. Cohorts collected were: i) 39 matched pairs of primary breast cancer and brain metastases; ii) 22 unmatched brain metastases from breast cancer; iii) 11 brain metastases from non-breast sites (one melanoma, one colorectal, six lung, one prostate and two renal cell carcinomas); and iv) 26 tumor samples (primary breast cancer and metastases to multiple sites, including brain) from six autopsy cases of patients who died of metastatic breast cancer (the primary breast cancer from one case was not available). The tumors were reviewed by three pathologists (LDS, MC and SRL) and analyzed by immunohistochemistry and chromogenic *in situ* hybridization (CISH) on tissue microarrays. Immunohistochemistry for EGFR, HER2, HER3, HER4, CD44 and CD24 was also done on whole sections.

Gene expression analysis

RNA was extracted from FFPE samples and the expression of 512 cancer related genes was analyzed using the DASL assay (cDNA-mediated annealing, selection extension and ligation, Illumina Inc., San Diego, California, USA) [25]. All data and protocols for DASL analysis can be found at the Gene Expression Omnibus repository (Accession number GSE14690) (see also additional file 1). Real-time PCR using TaqMan® gene expression assays (Applied Biosystems, Inc, Carlsbad, California, USA) and immunohistochemistry were performed to validate the expression of specific genes.

Somatic mutation analysis

Twelve matched pairs of primary breast tumors and corresponding brain metastases, nine non-breast brain metastases and 26 tumor samples from the six autopsy cases were subjected to primer extension and MALDI-TOF mass spectrometry using the OncoCarta® Panel Assay v1.0 (Sequenom Inc., San Diego, California, USA) of 238 mutations in 19 oncogenes [26]. All mutations in samples for which there was sufficient DNA remaining were validated by High Resolution Melt (HRM) [27] analysis, iPLEX (using newly designed PCR and extension primers that differed from the OncoCarta primers), repeat OncoCarta analysis, and/or direct sequencing if the Mutant Allele Proportion (MAP) was >30% (Table 1 and Additional file 2, Table S2). In addition, we were able to validate the *EGFR* E746_A750del mutation in four cases with a mutation-specific antibody [28].

Results

Clinical and pathological features

The median age at diagnosis was 48.5 years and the median time for the development of brain metastasis was 3.5 years. All but one of the series of primary breast cancers and all brain metastases were grade 3 invasive ductal carcinomas-no specific type (IDC-NST) [29]. The

Table 1 Somatic mutations identified by OncoCarta and ER, PgR and HER family of receptors assessment

Matched breast primary-brain metastasis pairs											
Case ID#	**Site**	**ER - PgR- HER 1-2-3-4**	***EGFR***		***NRAS***		***PIK3CA***				
			Mutation	**MAP**	**Mutation**	**MAP**	**Mutation**	**MAP**			
1	**brain**	ER-, PgR-, HER1-, HER2+, HER3-, HER4-									
	breast	ER-, PgR-, HER1-, HER2+, HER3-, HER4-									
2	**brain**	ER-, PgR-, HER1-, HER2-, HER3+, HER4-			Q61R$^{O, H, I, S}$	39.50%					
	breast	ER-, PgR-, HER1-, HER2-, HER3+, HER4-			Q61R$^{O, H, I, S}$	38.30%					
4	**brain**	ER-, PgR+, HER1+, HER2-, HER3-, HER4-									
	breast	ER-, PgR+, HER1+, HER2-, HER3-, HER4-									
6	**brain**	ER-, PgR+, HER1+, HER2-, HER3-, HER4-									
	breast	ER-, PgR+, HER1+, HER2-, HER3-, HER4-									
7	**brain**	ER-, PgR-, HER1+, HER2-, HER3-, HER4-			Q61R$^{I, S}$	34.4%					
	breast	ER-, PgR-, HER1+, HER2-, HER3-, HER4-			Q61R$^{I, S}$	34.1%					
8	**brain**	ER-, PgR-, HER1-, HER2+, HER3+, HER4-									
	breast	ER-, PgR-, HER1-, HER2+, HER3-, HER4-									
9	**brain**	ER-, PgR-, HER1-, HER2+, HER3-, HER4-					H1047R^{S}	79.50%			
	breast	ER-, PgR-, HER1-, HER2+, HER3-, HER4-					H1047R^{S}	79.50%			
10	**brain**	ER-, PgR-, HER1+, HER2-, HER3+, HER4-					E545K$^{H, NVP}$	23.40%			
	breast	ER-, PgR-, HER1+, HER2-, HER3-, HER4-					E545K$^{H, NVP}$	18.20%			
11	**brain**	ER-, PgR-, HER1-, HER2+, HER3-, HER4+									
	breast	ER-, PgR-, HER1-, HER2+, HER3-, HER4+									
12	**brain**	ER-, PgR+, HER1-, HER2-, HER3+, HER4-									
	breast	ER-, PgR+, HER1-, HER2-, HER3+, HER4-									
13	**brain**	ER-, PgR-, HER1+, HER2-, HER3-, HER4-									
	breast	ER-, PgR-, HER1+, HER2-, HER3-, HER4-	N771_P772>SVDNR	12.10%							
14	**brain**	ER-, PgR-, HER1+, HER2-, HER3-, HER4-									
	breast	ER-, PgR-, HER1+, HER2-, HER3-, HER4-									

Unmatched brain metastases from primary lung, colon, melanoma and kidney tumours												
Case ID#	**Site**	**ER - PgR- HER 1-2-3-4**	***EGFR***		***HRAS***		***KRAS***		***NRAS***		***PIK3CA***	
			Mutation	**MAP**	**Mutation**	**MAP**	**Mutation**	**MAP**	**Mutation**	**MAP**	**Mutation**	**MAP**
D2	**melanoma**	n.a.									E545K$^{H, I, Y}$	30.80%
D3	**colon**	n.a.					G12C^{S}	38.90%				
D4	**lung**	n.a.	E746_A750del^{A}	21.00%								
D5	**lung**	n.a.										

Table 1 Somatic mutations identified by OncoCarta and ER, PgR and HER family of receptors assessment *(Continued)*

D6	**lung**	n.a.	E746_A750del$^{A, NVI}$	14.40%	G13S^{I}	17.30%	G12C^{I,S}	35.70%	
D7	**lung**	n.a.					G12C$^{\mathbf{O;I}}$	9.70%	
D8	**lung**	n.a.				G12C^{S}	39.90%		
D9	**lung**	n.a.						E545K^{H}	13.30%
D10	**kidney**	n.a.	E746_A750del$^{A, I}$	9.10%			G12C$^{\mathbf{I, S}}$	35.20%	

A, validated by immunohistochemistry using a mutation-specific antibody; ER, estrogen receptor; H, validated by High Resolution Melt analysis; I, validated by iPLEX; ID, case number identification; MAP, Mutant Allele Proportion estimated by OncoCarta; NVI, not validated by iPLEX; NVP, no further validation possible because no DNA remained; O, validated by repeat OncoCarta; PgR, progesterone receptor; S, validated by sequencing; Y, sequencing did not work for this sample; n.a., not accessed.

remaining tumor pair was a grade 2 mucinous carcinoma. The autopsy samples comprised four grade 3 and one grade 2 IDC-NST.

ER, PgR, HER2, 'Basal' markers and stem cell markers (non-autopsy cases)

Immunohistochemistry data are summarized in Figure 1A, B (see also additional file 2, Table S1 and Figure S1). It was noteworthy that 60% and 76% of the tumors were negative for ER and PR, respectively, with complete concordance between primary and metastases. Seventy-seven percent (77%) and 81% of the unmatched brain metastases were also ER and PR negative, respectively. Twenty percent (20%) and 19% of the primary breast tumors and metastases, respectively, had correlated over-expression of HER2 (3+ staining) and all of these showed gene amplification using CISH. Twenty percent (20%) of the unmatched metastases were also HER2+. Fifty-six percent (56%) of the primary tumors and 48% of the matched metastases were triple negative and of these, 60% were positive for at least one of the basal markers respectively (CK14, CK5/6, CK17, EGFR and SMA). Overall, 54% of the primary and 60% of the metastases were of *basal* phenotype (irrespective of ER, PR and HER2 status), confirming enrichment in this cohort over the normal distribution in breast cancer [8]. Noteworthy, EGFR staining was seen mainly in the periphery of the tumor where there was contact with non-neoplastic brain parenchyma [30]. A higher proportion of brain metastases had a putative stem cell-like phenotype ($CD44^{+}/CD24^{-}$) compared to the primaries, 55% versus 25%, (Figure 1A). Fifty-one percent (51%) of the primary tumors had a Ki-67 index higher than 10% in contrast to matched and unmatched metastases that had 86% and 85% of samples with index higher than 10%.

Gene expression profiling

The availability of good quality RNA and stringent filtering of the DASL data yielded gene expression profiling data on 37/61 brain metastases from breast cancer (15/39 from matched pairs and 22/22 from unmatched metastases) and 15 matched primaries. Unsupervised analysis highlighted a strong similarity between primary tumors and their matched metastases (Figure 2A). Only 20 genes were differentially expressed between the matched primaries and metastases. This may be a consequence of the overall strong similarity between primaries and metastases [31] coupled with the sample size (n = 30) and number of genes analyzed (n = 512 cancer genes in the DASL panel) [32]. Comparison between primaries and all metastases (matched and unmatched) identified 27 statistically significant, differentially expressed genes (Figure 2B). Supplementary Figure 2

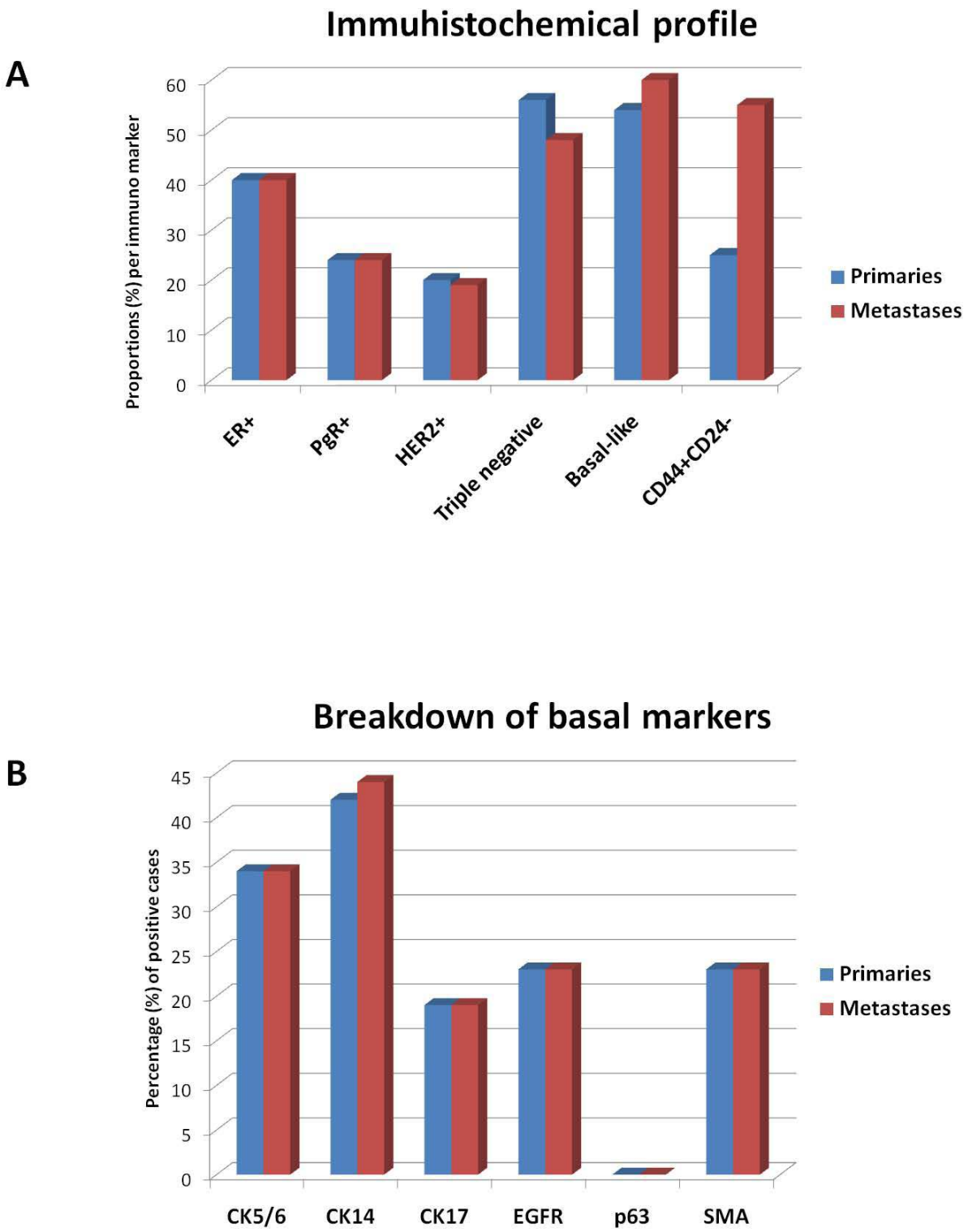

Figure 1 Immunohistochemical profile of primary breast and brain metastases. **A** - Immunohistochemical analysis of matched primary breast and brain metastases. The graph depicts percentages of positive cases in each category. ER and PR were considered positive when >10% cells showed staining, HER2 was considered positive when IHC showed 3+ staining (>30% positive cells) or CISH showed gene amplification. Triple negative tumors were negative for ER, PR and HER2. CD44+/CD24- immunohistochemistry was assessed on serial sections and positivity was expression in >10% cells. **B** - Breakdown of basal markers. A tumor was regarded as *basal* if any of the following markers were positive (CK5/6, CK14, CK17, p63, SMA, and EGFR) with >10% cells showed staining.

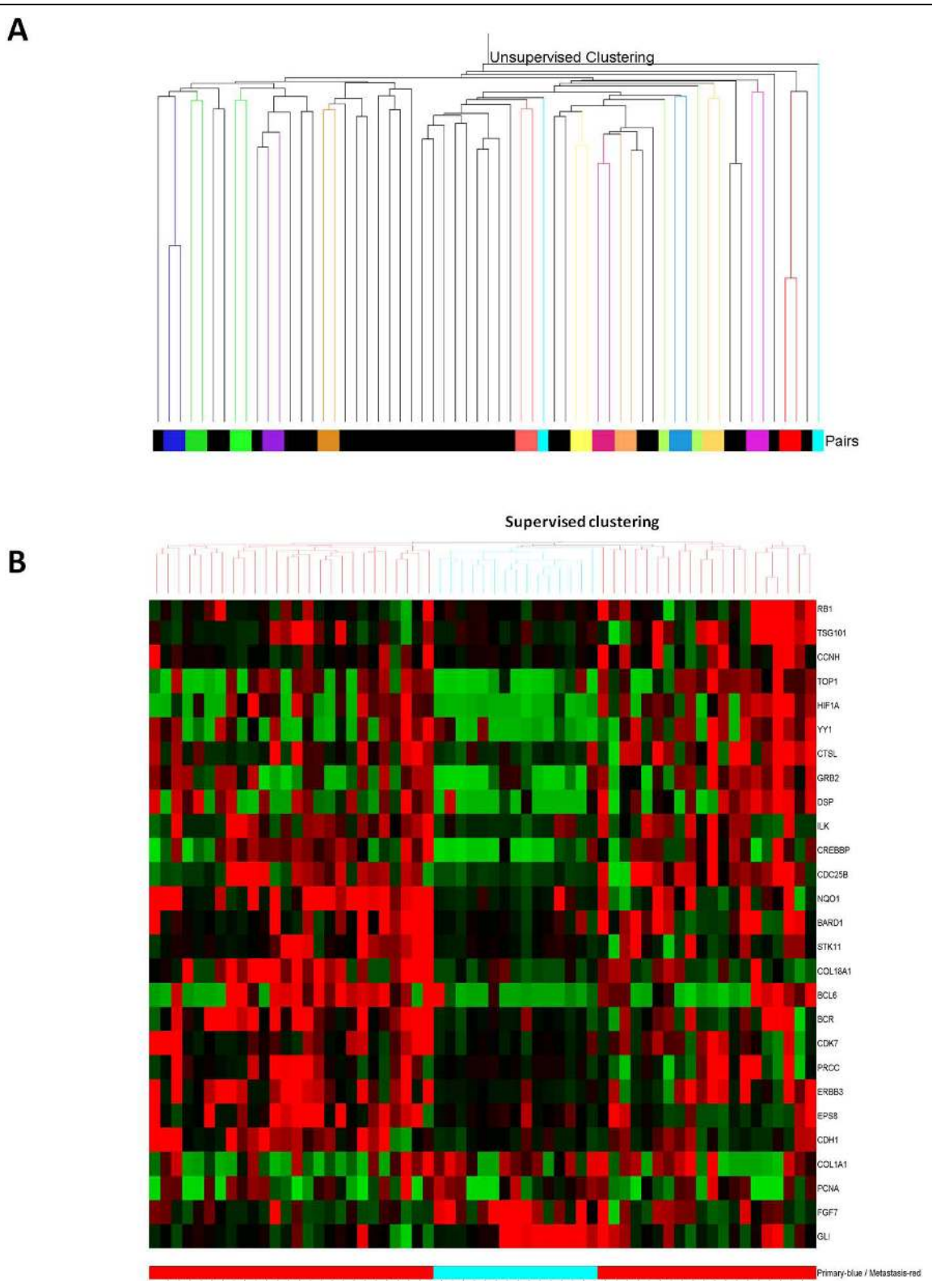

Figure 2 Gene expression profiling of brain metastases. **A** - Unsupervised hierarchical clustering of DASL gene expression data from 22 unmatched (black color bar) and 15 matched primary and brain metastases (other colors bars). Thirteen out of 15 matched samples are clustering together. **B** - Heatmap and dendogram showing clustering of the samples based on the 27 genes differentially expressed between primary tumors (blue line bar) and brain metastases (red line bar).

(see Additional file 2, Figure S2) depicts principal component analysis showing good separation of the primaries and metastases using this 27-gene list. All 20 genes identified in the matched pair analysis were part of this 27-gene set. Among this 20-gene set, were *HER3* and one of its downstream target molecules *GRB2* [33], hypoxia related molecule *HIF1-alfa*, MAPKinase cascade related protein *CREBBP*, cell cycle regulator RB1 and proliferation related genes *CCNH, CDK7* and *CDC25B*. Since the brain is rich in neuregulin 1 [34,35] and this is a ligand for HER3, we hypothesized that the neuregulin-HER3 activation was important in allowing breast cancer cells to colonize the brain.

HER family receptors and downstream molecules expression

HER3, EGFR, HER2, HER4 and *HIF1-alfa* expression was assessed using quantitative RT-PCR (see Additional file 2, Figure S3) in 12 matched breast/brain samples for which DASL data and RNA were available. Similar to the DASL data, 10 cases showed increased fold change by RT-PCR of *HER3* gene expression relative to their matched primaries ranging from 1.12 to 5.8 and with an average of 2.4. Immunohistochemistry for HER3 was similar, showing positivity in 11/37 (29.7%) of the primary tumors, 22/37 (59%) of the matched metastases and 13/21 (62%) of the unmatched brain metastases (P = 0.019). In agreement, phosphorylated HER3 confirmed more frequent activation in the brain metastases, with positivity in 14/37 (37%) of the primary tumors, 24/37 (64%) of the matched metastases and 18/21 (85%) of the unmatched brain metastases (P = 0.046) (see Additional file 2, Table S1 and Figure S1).

Immunohistochemistry for GRB2, HIF1-alfa and phosphorylated ERK1/2, JNK1/2, ERK5 and p38 also demonstrated increased activation in the metastases compared to the primary tumors; (see Additional file 2, Table S1 and Figure S1). In contrast, phosphorylated AKT was equally high in both the primaries and metastases (see Additional file 2, Table S1). Interestingly, the non-breast derived brain metastases showed similarly high activation of the MAPK pathway together with over-expression (3+ stain) of EGFR (in 9/11 (81%) metastases (a prostate and one colon carcinoma did not) but in the absence of HER3 activation (0/11) (see Additional file 2, Table S1).

Somatic mutation analysis

OncoCarta analysis identified mutations in the brain metastases from primary breast cancers (non-autopsy cases) in *NRAS* (2/12 - 17%), and *PIK3CA* (2/12 - 17%) (Table 1 and Figure 3). Mutations were also identified in brain metastases from non-breast primaries in *EGFR* (3/9 - 33%; two lung and one kidney), *HRAS* (1/9 - 11%; lung), *KRAS* (2/9 - 22%; one colon and one lung), *NRAS* (3/9 - 33%; two lung and one kidney) and *PIK3CA* (2/9 - 22%; one melanoma and one lung).

Mutant Allele Proportions (MAPs) ranged from 9% to 80%. All these mutations were validated by immunohistochemistry (using a specific antibody raised against the protein with the *EGFR* E746_A750del mutation) or sequencing except for one each in *EGFR, HRAS* (validated by iPLEX), *NRAS* and *PIC3CA* (*validated* by HRM), where the estimated mutant allele proportion was less than 15%, and two in *PIK3CA* in which there was insufficient good quality DNA remaining to obtain sequence data. *EGFR* G719 S appeared to be found frequently by OncoCarta but could not be detected by iPLEX, using independent PCR and extension primers. The OncoCarta false-positive result appeared to be due to hairpin formation of the extension primer that occurred frequently when archival DNA was used as a template, and the yield was low.

Except for one *EGFR* mutation (Case #13; Table 1), the same somatic mutations were observed in the brain metastases with similar MAPs as in the matched primary breast tumors. It was noteworthy that the four matched pairs harboring somatic mutation in *NRAS* or *PIK3CA* also overexpressed a member of the HER family. For example, matched pair #2 had a mutation in *NRAS* and showed over-expression of HER3, matched pair #7 had a mutation in *NRAS* and showed over-expression of HER1, matched pair #9 had a mutation in *PIK3CA* and amplification of HER2 and matched pair #10 had a mutation in *PIK3CA* and overexpression of HER1 (Table 1).

Among the autopsy samples of cases with primary breast cancer, we found mutations in *EGFR* in one liver and one lymph node metastases, and a mutation in *PIK3CA* in all the samples from one case, and in a liver metastasis from another (see Additional file 2, Table S2). One *EGFR* and one *PIK3CA* mutation could be verified by sequencing or immunohistochemistry but lack of good quality DNA, and additional mutation-specific antibodies, prohibited validation of the others. All the samples from one case had the same mutation at similar MAPs (*PIK3CA* H1074R in Patient #2).

We identified *HRAS* and *PIK3CA* mutations in the basal breast cancer cell lines SUM 159 and BT20. The mutations with MAPs >25% have been reported before [19,20]: *HRAS* G12 D (MAP 53.2% in SUM159) and *PIK3CA* H1047L (MAP 50.0% in SUM159) and P539R (MAP 43.8% in BT20) but we also identified *HRAS* Q61K at MAP 24.6% in SUM159 and *HRAS* Q61K at MAP 14.1%, and *PIK3CA* H1047R at MAP 44.4% in BT20. In addition, we were also able to show that all of the mutations with MAPs >25% were present in mammospheres derived from these cell lines.

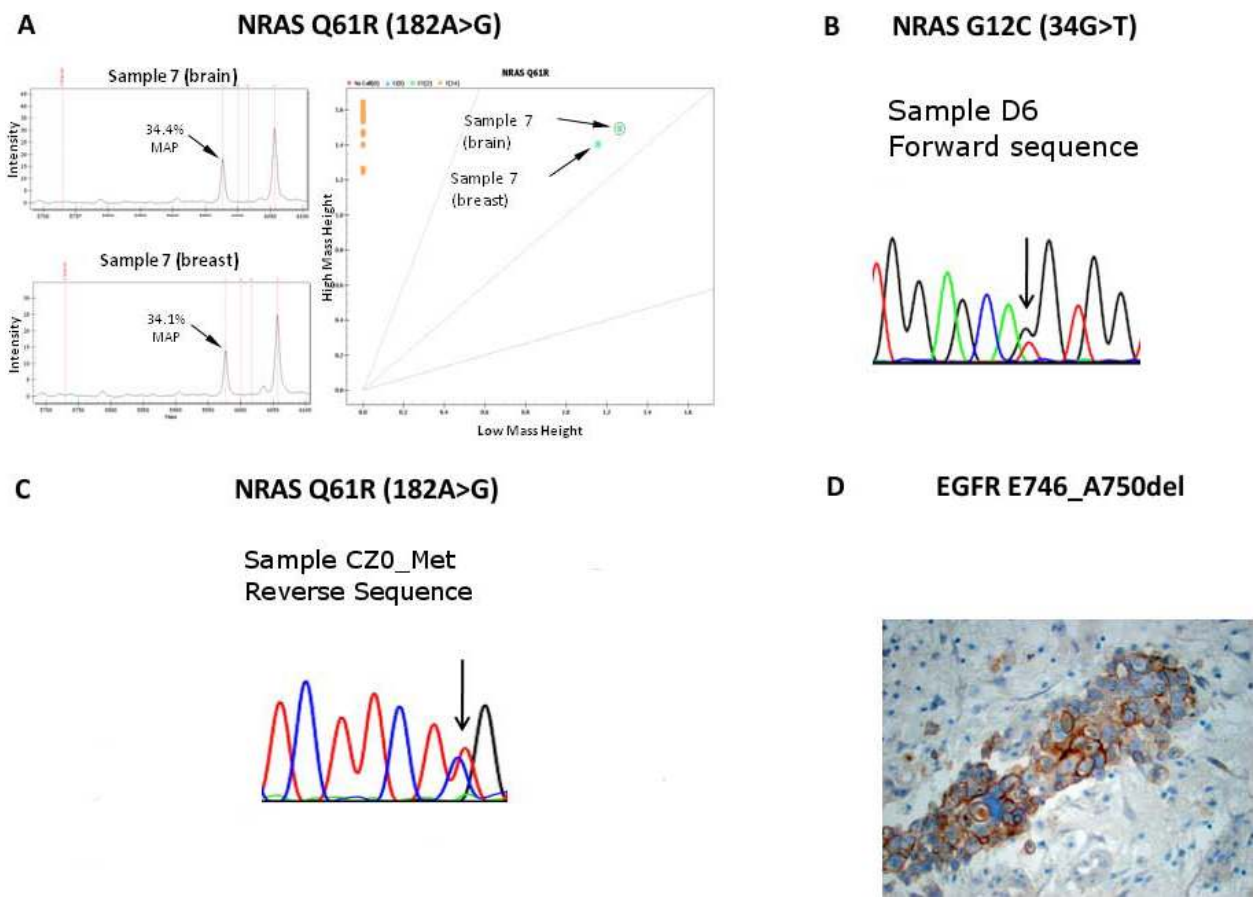

Figure 3 Oncocarta and validation mutation analyses. **A)**. Example of *NRAS* Q61R mutation identified by OncoCarta in matched pair sample #7 showing representative spectra and cluster plot. **B)** Sequence validation of *NRAS* G12C, sample D6 - lung metastasis. **C)** Sequence validation of *NRAS* Q61R, breast and brain metastasis from sample #2. **D)** Immunohistochemistry of brain metastasis (sample D4) with antibody specific to *EGFR* E746_A750del showing staining in the tumor but not the surrounding brain tissue.

Discussion

We have collected a unique set of clinical material through collaborations with multiple institutions around the world and involving brain metastases which are rarely excised. The analysis of this resource has led to the development of hypotheses regarding the mechanisms of breast cancer colonization of the brain (Figure 4). The set of tumor samples is enriched for triple negative/basal breast cancers which is consistent with the findings of an increased propensity for basal breast cancers to metastasize to the brain [3,9,36]. An association between CD44+/CD24- frequency and a basal tumor phenotype has already been reported [37] and interestingly we observed an increased frequency of CD44+/CD24- cells in the brain metastases compared to their matched primaries. CD44+/CD24- cells have been reported to have stem cell properties and increased *in vivo* tumorigenicity [38] and the increased frequency seen in brain metastases may support this. Alternatively, this may reflect selection as a result of a high content of hyaluron, the ligand for CD44, within the brain microenvironment [39,40]. Hence, this could be an important factor in breast cancer colonization of the brain and therefore a potential axis for future therapeutic intervention [41].

In this study, brain metastases of breast cancer expressed all members of the HER family of tyrosine kinase receptors. HER2 was amplified and overexpressed in 20% of brain metastases, EGFR was overexpressed in 21% of brain metastases, HER3 was overexpressed in 60% of brain metastases and HER4 was overexpressed in 22% of brain metastases and generally mutually exclusive (Table 1). Interestingly, HER3 expression was increased in breast cancer cells residing in the brain. Neuregulin 1, the ligand for this receptor, is abundantly expressed in the brain [34,35] and is released by a variety of mechanisms including the presence of hypoxia [42]. Consistent with this, we observed the increased expression of *HIF-1alfa* in the brain metastases, likely to reflect the local hypoxic environment [43]. Increased

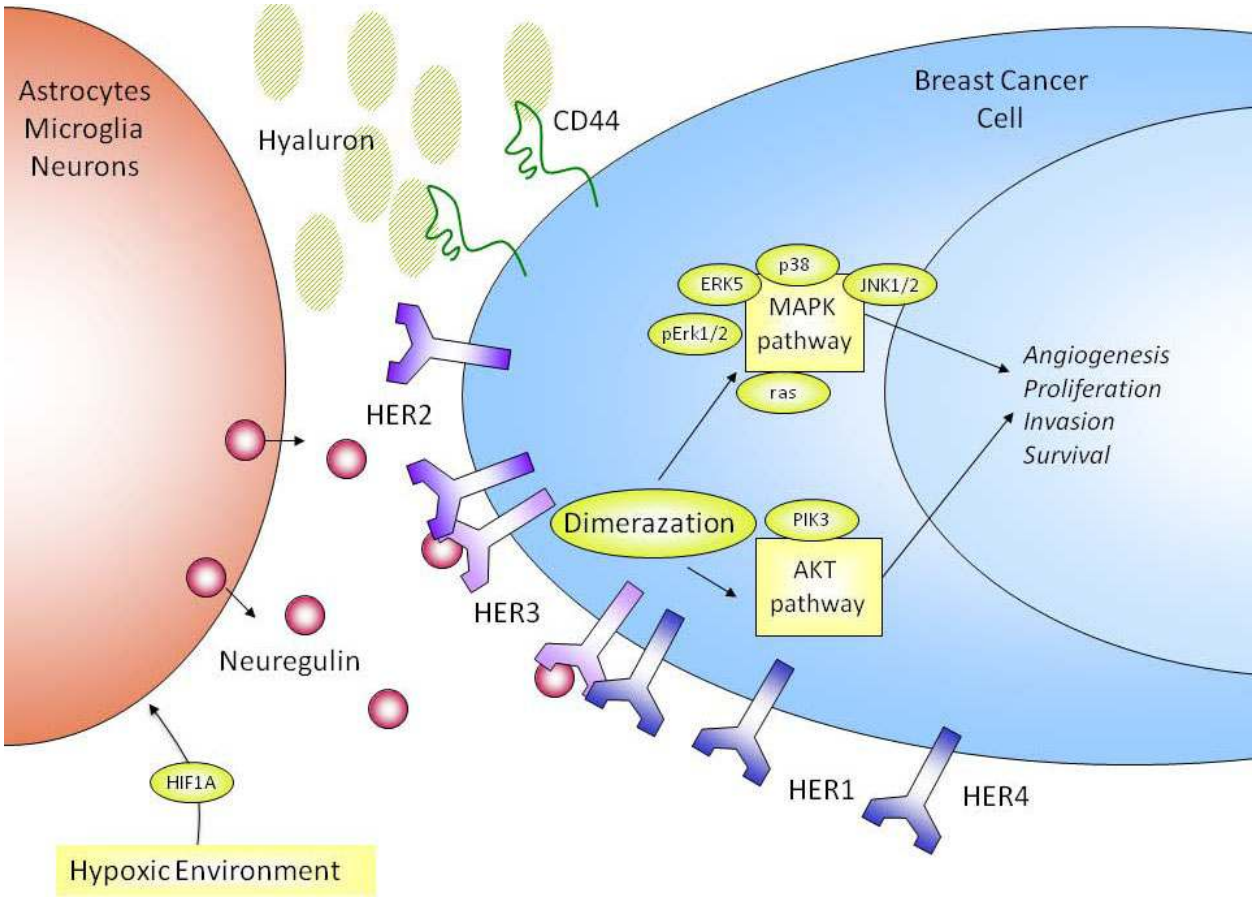

Figure 4 Hypothetical mechanism of breast cancer cell colonization of the brain parenchyma. Hypoxic conditions, (HIF1a) can mediate the elease of neuregulin 1 from neuronal cells. Neuregulin 1 is the ligand for HER3 and on binding activates the heterodimerisation of HER3-HER2, HER3-HER4 and/or HER3-HER1, leading to downstream activation of the MAPK and AKT pathways. MAPK/AKT pathways activation is related to survival, invasion, proliferation and angiogenesis. A second mechanism of colonization may relate to the enriched expression of CD44 breast cancer cells in the brain. The brain microenvironment is rich in hyaluron, the ligand for CD44, and so upon activation a series of responses maybe triggered, including cell motility.

activation of both HER3 and downstream molecules (GRB2, ERK5, ERK1/2, JNK1/2, p38) was also observed in the brain metastases. These findings prompted us to hypothesize that neuregulin/HER3 activation is an important mechanism for breast cancer cell colonization of the brain (Figure 4). As a further support to this hypothesis, increased HER3 expression has also been reported in brain metastases of lung cancer [44].

We investigated whether this association was generic to all brain metastases and found activation of the MAPK pathway in all 11 non-breast metastases to the brain. Whilst HER3 was not activated in these tumors, 9/11 tumors showed over-expression of EGFR. It has recently been shown, using animal models, that EGFR ligands mediate breast cancer metastasis to the brain and that this was abrogated by the use of EGFR inhibitor cetuximab [14]. The combination of lapatinib and trastuzumab has been shown to have a synergistic, antiproliferative effect against ErbB2-positive breast cancer cells *in vitro* [45]. It is possible, therefore, that a combination of anti-HER therapies could be effective in the treatment of both breast and non-breast metastases to the brain.

In order to activate downstream signaling pathways, HER3 requires heterodimerization with other members of the HER family following binding by neuregulin [46] and even basal levels of the other HER proteins may be sufficient to participate in the activation of these pathways. Hence, combination therapy against the HER family, even in the absence of over-expression or amplification of HER2, may be of clinical benefit for a larger proportion of breast cancer patients such as those with HER2 negative disease. Recently, a study showed benefits for a small group of HER2-negative patients in the phase III National Surgical Adjuvant Breast and Bowel Project (NSABP) B-31 trial that were HER2 negative by

FISH and had less than 3+ staining intensity by HercepTest® (Dako, Carpinteria, CA, USA) [47]. Furthermore, another study suggested that the spectrum of patients who may benefit from trastuzumab-based therapies could be expanded to include patients with metastatic breast cancer without HER-2 amplification but who express transmembrane neuregulin, the ligand of HER3 [48]. It has also been reported in non-HER2 overexpressing xenograft models of prostate and breast cancer that pertuzumab, an inhibitor of HER3/HER2 heterodimerization, can inhibit tumor growth [49].

For the first time, we have identified somatic mutations in genes related to the AKT/MAPK signaling pathways, such as *EGFR*, *PIK3CA*, *KRAS*, *HRAS* and *NRAS*, in brain metastases of breast cancer and other types of cancer. In addition, we have analyzed multiple autopsy samples from six cases that had a primary breast cancer, and found additional *EGFR* and *PIK3CA* mutations in breast cancers that metastasized to various sites including the brain. Thus, simply targeting the HER family of receptors may not be sufficient for complete treatment response. This analysis highlights additional *actionable* targets [50] that may prove effective for the treatment of some brain metastasis, such as PI3 kinase inhibitors.

Taken together, these findings are striking and show another facet of the cell evolution landscape [51], highlighting the possibility of cancer cells resisting targeted treatment to molecules such as HER2 or EGFR by acquiring oncogenic mutations in downstream pathways. This has been shown *in vitro* with activating PIK3CA mutation [23] and herein we demonstrate an *in vivo* example of this possible scenario using human tumors. In another clinical angle, patients currently treated with the anti-EGFR monoclonal antibodies cetuximab and panitumumab can also acquire resistance to this therapy due to downstream mutations in the *ras* gene [24]. Interestingly, animal models have suggested that downstream NF-kappaB inhibitory drugs may play a role in the treatment of patients with defined mutations in *KRAS* [52].

Interestingly the Mutant Allele Proportion (MAP) was sometimes as low as 10%. Such low proportion mutations, which would often be missed by direct sequencing could reflect the presence of stromal (or brain) contamination in the samples, tumor heterogeneity and amplification or deletion of the mutant or wild type alleles. However, the fact that the same MAP was often observed in both the primary and the brain metastasis, and in the multiple samples from an autopsy case, might suggest that these metastases were not seeded by a single cell but by groups of cells from the primary tumor. This has also been shown by next generation sequencing, whereby the mutant allele frequency for some mutations was similar between a basal-like primary breast cancer and its matched brain metastasis [53]. However, it is also evident that significant genomic evolution occurs during metastasis, since most mutations identified in this metastasis, and one from a primary lobular breast cancer, were more prevalent in the metastasis than in the respective primary tumours [53,54]

Conclusions

In conclusion, we provide evidence to support a role of HER3 and other HER family receptors in the ability of cancer cells to colonize the brain. The data are intriguing and support the possibility that tumors with low expression of HER2 may respond to trastuzumab, lapitinib or combinations of HER family receptor inhibitors since even basal levels may enhance the signaling through homo/hetero-dimerization of the other receptors. However, caution should be exercised because of the possible presence of downstream oncogenic mutations that may drive treatment resistance. These therapeutic modalities may therefore add another dimension to the treatment of triple negative and basal-like cancers where currently, no targeted therapy is available.

Acknowledgements

Leonard Da Silva and Ana Cristina Vargas are recipients of PhD Fellowships from the Ludwig Institute of Cancer Research. Leonard Da Silva is enrolled with the *"Universidade Federal de São Paulo, Escola Paulista de Medicina, Curso de Pós-Graduação, Doutorado, Departamento de Anatomia Patológica, São Paulo, Brazil"*. Peter Simpson is a recipient of a fellowship from the National Breast Cancer Foundation. Georgia Chenevix-Trench and KumKum Khanna are Senior Principal Research Fellows of the NHMRC. RLB is a Cancer Institute NSW Fellow. We also acknowledge the help of staff within anatomical pathology, RBWH, Brisbane, the animal house facility at UQ AIBN, Brisbane, Casey Wright from the Thoracic Research Laboratory, School of Medicine, at the UQ, and Clay Winterford and his staff from the UQ/QIMR Histotechnology facility, and Macky Edmundson in the sequencing facility at QIMR. We would like to thank Sequenom Inc. for providing the primer sequences used for HRM, and, in particular, we thank Darryl Irwin for his help.

Additional material

Additional file 1: Supplementary methodologies. This file contains information of how the morphological review and TMA creation were performed. It also contains information on protocols for immunohistochemistry and chromogenic *in situ* hybridization, RNA extraction and Real-Time RT-PCR, DASL gene expression profiling, cell line analysis and culture, oncoCarta somatic mutation analysis protocols, high resolution melt analysis and iPLEX genotyping protocols.

Additional file 2: Supplementary results. This file contains tables and figures regarding all immunohistochemistry data, extra gene expression and mutation results, and HER family gene expression by RT-PCR.

Abbreviations

CISH: chromogenic *in situ* hybridization; DASL: cDNA-mediated Annealing, Selection, extension, and Ligation; EGFR: epidermal growth factor receptor; ER: estrogen receptor; FFPE: formalin fixed-paraffin embedded; GEO: Gene Expression Omnibus; HER: human epidermal growth factor receptor; HRM: High Resolution Melt; IDC: invasive ductal carcinoma; MAPs: Mutant Allele Proportions; NSABP: National Surgical Adjuvant Breast and Bowel Project; NST: non-specific type; PgR: progesterone receptors.

Author details

[1]Molecular & Cellular Pathology, The University of Queensland Centre for Clinical Research, & School of Medicine, Building 918/B71, RBWH complex, Brisbane, 4029, Australia. [2]Cancer Genetics and Molecular Pathology, The Queensland Institute of Medical Research, 300 Herston Road, Brisbane, 4006, Australia. [3]Departamento de Anatomia Patológica, Universidade Federal de São Paulo, EPM, 754 Rua Napoleão de Barros, São Paulo, 04024-000, Brazil. [4]Biomolecular and Biomedical Science, Griffith University, 170 Kessels Road, Brisbane, 4011, Australia. [5]Centre for Magnetic Resonance, The University of Queensland, St Lucia, Brisbane, 4072, Australia. [6]Lembaga Eijkman, Eijkman Institute, Diponegoro 69, Jakarta, 10430, Indonesia. [7]Departamento de Patologia, Instituto Nacional de Câncer, 23 Praça Cruz Vermelha, Rio de Janeiro, 20230-130, Brazil. [8]Departamento de Patologia, Laboratório Salomão & Zoppi, 48 Rua Correia Dias, São Paulo, 04104-000, Brazil. [9]Department of Pathology, Medical Faculty of Charles University in Plzen, Husova 3, 306 05, Czech Republic. [10]Sydney West Area Health Service, Institute of Clinical Pathology and Medical Research, University of Sydney, Darcy Road, Sydney, 2145, Australia. [11]Translational Oncology, Sydney West Area Health Service, Westmead Millennium Institute, University of Sydney, Darcy Road, Sydney, 2145, Australia. [12]Department of Pathology, Peter MacCallum Cancer Centre, St Andrews Pl, East Melbourne, 3002, Australia. [13]Queensland Brain Institute, The University of Queensland, St Lucia, Brisbane, 4072, Australia. [14]Signal Transduction, The Queensland Institute of Medical Research, 300 Herston Road, Brisbane, 4006, Australia. [15]Pathology Queensland: The Royal Brisbane & Women's Hospital, Herston Road, Brisbane, 4029, Australia. [16]Current address - University of Florida, McKnight Brain Institute,100 S. Newell Drive, Gainesville, 32611, USA.

Authors' contributions

LDS analysed the immunohistochemical markers, accrued and collated the data, carried out statistical and gene expression analysis and drafted the manuscript. PK and ACV analysed immunohistochemical markers, and accrued and collated the data. NW, CES and PTS supervised gene expression analyses and drafted the manuscript. EP, PF, AS, MF, RB, MB and MC identified patients with brain metastases in their institutions, collected samples and performed initial tumor classification. LR, SP, PK and AL performed immunohistochemistry and participated in the construction of TMAs. KK, NK, BJM and BR participated in the study design. SB, SH and JB performed mutation analyses. HD, AD and SF performed validation of EGFR mutations. GCT and SRL conceived the study, supervised the experiments and drafted the manuscript.

Competing interests

Leonard Da Silva and Sunil Lakhani hold an USA registered patent relating to the data in this manuscript. All the other authors declare no conflict of interest.

Received: 14 March 2010 Revised: 15 June 2010 Accepted: 6 July 2010
Published: 6 July 2010

References

1. Lin NU, Bellon JR, Winer EP: **CNS metastases in breast cancer.** *J Clin Oncol* 2004, **22**:3608-3617.
2. Weil RJ, Palmieri DC, Bronder JL, Stark AM, Steeg PS: **Breast cancer metastasis to the central nervous system.** *Am J Pathol* 2005, **167**:913-920.
3. Hicks DG, Short SM, Prescott NL, Tarr SM, Coleman KA, Yoder BJ, Crowe JP, Choueiri TK, Dawson AE, Budd GT, Tubbs RR, Casey G, Weil RJ: **Breast cancers with brain metastases are more likely to be estrogen receptor negative, express the basal cytokeratin CK5/6, and overexpress HER2 or EGFR.** *Am J Surg Pathol* 2006, **30**:1097-1104.
4. Shmueli E, Wigler N, Inbar M: **Central nervous system progression among patients with metastatic breast cancer responding to trastuzumab treatment.** *Eur J Cancer* 2004, **40**:379-382.
5. Tham YL, Sexton K, Kramer R, Hilsenbeck S, Elledge R: **Primary breast cancer phenotypes associated with propensity for central nervous system metastases.** *Cancer* 2006, **107**:696-704.
6. Arteaga CL: **ErbB-targeted therapeutic approaches in human cancer.** *Exp Cell Res* 2003, **284**:122-130.
7. Hudis CA: **Trastuzumab–mechanism of action and use in clinical practice.** *N Engl J Med* 2007, **357**:39-51.
8. Rakha EA, Reis-Filho JS, Ellis IO: **Basal-like breast cancer: a critical review.** *J Clin Oncol* 2008, **26**:2568-2581.
9. Fulford LG, Reis-Filho JS, Ryder K, Jones C, Gillett CE, Hanby A, Easton D, Lakhani SR: **Basal-like grade III invasive ductal carcinoma of the breast: patterns of metastasis and long-term survival.** *Breast Cancer Res* 2007, **9**: R4.
10. Luck AA, Evans AJ, Green AR, Rakha EA, Paish C, Ellis IO: **The influence of basal phenotype on the metastatic pattern of breast cancer.** *Clin Oncol (R Coll Radiol)* 2008, **20**:40-45.
11. Paget S: **The distribution of secondary growths in cancer of the breast.** *Cancer Metastasis Rev* 1989, **8**:98-101.
12. Minn AJ, Gupta GP, Siegel PM, Bos PD, Shu W, Giri DD, Viale A, Olshen AB, Gerald WL, Massague J: **Genes that mediate breast cancer metastasis to lung.** *Nature* 2005, **436**:518-524.
13. Minn AJ, Kang Y, Serganova I, Gupta GP, Giri DD, Doubrovin M, Ponomarev V, Gerald WL, Blasberg R, Massague J: **Distinct organ-specific metastatic potential of individual breast cancer cells and primary tumors.** *J Clin Invest* 2005, **115**:44-55.
14. Bos PD, Zhang XH, Nadal C, Shu W, Gomis RR, Nguyen DX, Minn AJ, van de Vijver MJ, Gerald WL, Foekens JA, Massagué J: **Genes that mediate breast cancer metastasis to the brain.** *Nature* 2009, **459**:1005-1009.
15. Palmieri D, Bronder JL, Herring JM, Yoneda T, Weil RJ, Stark AM, Kurek R, Vega-Valle E, Feigenbaum L, Halverson D, Vortmeyer AO, Steinberg SM, Aldape K, Steeg PS: **Her-2 overexpression increases the metastatic outgrowth of breast cancer cells in the brain.** *Cancer Res* 2007, **67**:4190-4198.
16. Wood LD, Parsons DW, Jones S, Lin J, Sjöblom T, Leary RJ, Shen D, Boca SM, Barber T, Ptak J, Silliman N, Szabo S, Dezso Z, Ustyanksky V, Nikolskaya T, Nikolsky Y, Karchin R, Wilson PA, Kaminker JS, Zhang Z, Croshaw R, Willis J, Dawson D, Shipitsin M, Willson JK, Sukumar S, Polyak K, Park BH, Pethiyagoda CL, Pant PV, *et al*: **The genomic landscapes of human breast and colorectal cancers.** *Science* 2007, **318**:1108-1113.
17. Lin J, Gan CM, Zhang X, Jones S, Sjöblom T, Wood LD, Parsons DW, Papadopoulos N, Kinzler KW, Vogelstein B, Parmigiani G, Velculescu VE: **A multidimensional analysis of genes mutated in breast and colorectal cancers.** *Genome Res* 2007, **17**:1304-1318.
18. Stephens PJ, McBride DJ, Lin ML, Varela I, Pleasance ED, Simpson JT, Stebbings LA, Leroy C, Edkins S, Mudie LJ, Greenman CD, Jia M, Latimer C, Teague JW, Lau KW, Burton J, Quail MA, Swerdlow H, Churcher C, Natrajan R, Sieuwerts AM, Martens JW, Silver DP, Langerød A, Russnes HE, Foekens JA, Reis-Filho JS, van't Veer L, Richardson AL, Børresen-Dale AL, *et al*: **Complex landscapes of somatic rearrangement in human breast cancer genomes.** *Nature* 2009, **462**:1005-1010.
19. Hollestelle A, Nagel JH, Smid M, Lam S, Elstrodt F, Wasielewski M, Ng SS, French PJ, Peeters JK, Rozendaal MJ, Riaz M, Koopman DG, Ten Hagen TL, de Leeuw BH, Zwarthoff EC, Teunisse A, van der Spek PJ, Klijn JG, Dinjens WN, Ethier SP, Clevers H, Jochemsen AG, den Bakker MA, Foekens JA, Martens JW, Schutte M: **Distinct gene mutation profiles among luminal-type and basal-type breast cancer cell lines.** *Breast Cancer Res Treat* 2010, **121**:53-64.
20. **COSMIC - Catalogue of Somatic Mutations in Cancer.** [http://www.sanger.ac.uk/genetics/CGP/cosmic/].

21. Hu X, Stern HM, Ge L, O'Brien C, Haydu L, Honchell CD, Haverty PM, Peters BA, Wu TD, Amler LC, Chant J, Stokoe D, Lackner MR, Cavet G: **Genetic alterations and oncogenic pathways associated with breast cancer subtypes.** *Mol Cancer Res* 2009, **7**:511-522.
22. Hynes NE, Dey JH: **PI3K inhibition overcomes trastuzumab resistance: blockade of ErbB2/ErbB3 is not always enough.** *Cancer Cell* 2009, **15**:353-355.
23. Junttila TT, Akita RW, Parsons K, Fields C, Lewis Phillips GD, Friedman LS, Sampath D, Sliwkowski MX: **Ligand-independent HER2/HER3/PI3K complex is disrupted by trastuzumab and is effectively inhibited by the PI3K inhibitor GDC-0941.** *Cancer Cell* 2009, **15**:429-440.
24. Normanno N, Tejpar S, Morgillo F, De Luca A, Van Cutsem E, Ciardiello F: **Implications for KRAS status and EGFR-targeted therapies in metastatic CRC.** *Nat Rev Clin Oncol* 2009, **6**:519-527.
25. Fan JB, Yeakley JM, Bibikova M, Chudin E, Wickham E, Chen J, Doucet D, Rigault P, Zhang B, Shen R, McBride C, Li HR, Fu XD, Oliphant A, Barker DL, Chee MS: **A versatile assay for high-throughput gene expression profiling on universal array matrices.** *Genome Res* 2004, **14**:878-885.
26. Thomas RK, Baker AC, Debiasi RM, Winckler W, Laframboise T, Lin WM, Wang M, Feng W, Zander T, MacConaill L, Lee JC, Nicoletti R, Hatton C, Goyette M, Girard L, Majmudar K, Ziaugra L, Wong KK, Gabriel S, Beroukhim R, Peyton M, Barretina J, Dutt A, Emery C, Greulich H, Shah K, Sasaki H, Gazdar A, Minna J, Armstrong SA, *et al*: **High-throughput oncogene mutation profiling in human cancer.** *Nat Genet* 2007, **39**:347-351.
27. Krypuy M, Newnham GM, Thomas DM, Conron M, Dobrovic A: **High resolution melting analysis for the rapid and sensitive detection of mutations in clinical samples: KRAS codon 12 and 13 mutations in non-small cell lung cancer.** *BMC Cancer* 2006, **6**:295.
28. Yu J, Kane S, Wu J, Benedettini E, Li D, Reeves C, Innocenti G, Wetzel R, Crosby K, Becker A, Ferrante M, Cheung WC, Hong X, Chirieac LR, Sholl LM, Haack H, Smith BL, Polakiewicz RD, Tan Y, Gu TL, Loda M, Zhou X, Comb MJ: **Mutation-specific antibodies for the detection of EGFR mutations in non-small-cell lung cancer.** *Clin Cancer Res* 2009, **15**:3023-3028.
29. Ellis IO, Schnitt SJ, Sastre-Garau X, Bussolati G, Tavassoli FA, Eusebi V, Peterse JL, Mukai K, Tabar L, Jacquemier J, *et al*: **Invasive breast carcinomas.** *Pathology and Genetics of Tumours of the Breast and Female Genital Organs* Lyon: IARC PressTavassoli FA, Devilee P 2003, 13-59.
30. DiGiovanna MP, Lerman MA, Coffey RJ, Muller WJ, Cardiff RD, Stern DF: **Active signaling by Neu in transgenic mice.** *Oncogene* 1998, **17**:1877-1884.
31. Weigelt B, Hu Z, He X, Livasy C, Carey LA, Ewend MG, Glas AM, Perou CM, Van't Veer LJ: **Molecular portraits and 70-gene prognosis signature are preserved throughout the metastatic process of breast cancer.** *Cancer Res* 2005, **65**:9155-9158.
32. Kao LS, Green CE: **Analysis of variance: is there a difference in means and what does it mean?** *J Surg Res* 2008, **144**:158-170.
33. Schulze WX, Deng L, Mann M: **Phosphotyrosine interactome of the ErbB-receptor kinase family.** *Mol Syst Biol* 2005, **1**:2005.
34. Law AJ, Shannon Weickert C, Hyde TM, Kleinman JE, Harrison PJ: **Neuregulin-1 (NRG-1) mRNA and protein in the adult human brain.** *Neuroscience* 2004, **127**:125-136.
35. Pinkas-Kramarski R, Eilam R, Spiegler O, Lavi S, Liu N, Chang D, Wen D, Schwartz M, Yarden Y: **Brain neurons and glial cells express Neu differentiation factor/heregulin: a survival factor for astrocytes.** *Proc Natl Acad Sci USA* 1994, **91**:9387-9391.
36. Gaedcke J, Traub F, Milde S, Wilkens L, Stan A, Ostertag H, Christgen M, von Wasielewski R, Kreipe HH: **Predominance of the basal type and HER-2/neu type in brain metastasis from breast cancer.** *Mod Pathol* 2007, **20**:864-870.
37. Honeth G, Bendahl PO, Ringner M, Saal LH, Gruvberger-Saal SK, Lovgren K, Grabau D, Ferno M, Borg A, Hegardt C: **The CD44+/CD24- phenotype is enriched in basal-like breast tumors.** *Breast Cancer Res* 2008, **10**:R53.
38. Al-Hajj M, Wicha MS, Benito-Hernandez A, Morrison SJ, Clarke MF: **Prospective identification of tumorigenic breast cancer cells.** *Proc Natl Acad Sci USA* 2003, **100**:3983-3988.
39. Nandi A, Estess P, Siegelman MH: **Hyaluronan anchoring and regulation on the surface of vascular endothelial cells is mediated through the functionally active form of CD44.** *J Biol Chem* 2000, **275**:14939-14948.
40. Al Qteishat A, Gaffney JJ, Krupinski J, Slevin M: **Hyaluronan expression following middle cerebral artery occlusion in the rat.** *Neuroreport* 2006, **17**:1111-1114.
41. Marangoni E, Lecomte N, Durand L, de Pinieux G, Decaudin D, Chomienne C, Smadja-Joffe F, Poupon MF: **CD44 targeting reduces tumour growth and prevents post-chemotherapy relapse of human breast cancers xenografts.** *Br J Cancer* 2009, **100**:918-922.
42. Parker MW, Chen Y, Hallenbeck JM, Ford BD: **Neuregulin expression after focal stroke in the rat.** *Neurosci Lett* 2002, **334**:169-172.
43. Wang GL, Semenza GL: **Characterization of hypoxia-inducible factor 1 and regulation of DNA binding activity by hypoxia.** *J Biol Chem* 1993, **268**:21513-21518.
44. Sun M, Behrens C, Feng L, Ozburn N, Tang X, Yin G, Komaki R, Varella-Garcia M, Hong WK, Aldape KD, Wistuba II: **HER family receptor abnormalities in lung cancer brain metastases and corresponding primary tumors.** *Clin Cancer Res* 2009, **15**:4829-4837.
45. Konecny GE, Pegram MD, Venkatesan N, Finn R, Yang G, Rahmeh M, Untch M, Rusnak DW, Spehar G, Mullin RJ, Keith BR, Gilmer TM, Berger M, Podratz KC, Slamon DJ: **Activity of the dual kinase inhibitor lapatinib (GW572016) against HER-2-overexpressing and trastuzumab-treated breast cancer cells.** *Cancer Res* 2006, **66**:1630-1639.
46. Berger MB, Mendrola JM, Lemmon MA: **ErbB3/HER3 does not homodimerize upon neuregulin binding at the cell surface.** *FEBS Lett* 2004, **569**:332-336.
47. S Paik CK, Jeong J, Geyer CE, Romond EH, Mejia-Mejia O, Mamounas EP: **Benefit from adjuvant trastuzumab may not be confined to patients with IHC 3+ and/or FISH-positive tumors: Central testing results from NSABP B-31.** *ASCO Annual Meeting Proceedings (Post-Meeting Edition), Journal of Clinical Oncology* 2007, **25(18S)**:511.
48. de Alava E, Ocana A, Abad M, Montero JC, Esparis-Ogando A, Rodriguez CA, Otero AP, Hernandez T, Cruz JJ, Pandiella A: **Neuregulin expression modulates clinical response to trastuzumab in patients with metastatic breast cancer.** *J Clin Oncol* 2007, **25**:2656-2663.
49. Agus DB, Akita RW, Fox WD, Lewis GD, Higgins B, Pisacane PI, Lofgren JA, Tindell C, Evans DP, Maiese K, Scher HI, Sliwkowski MX: **Targeting ligand-activated ErbB2 signaling inhibits breast and prostate tumor growth.** *Cancer Cell* 2002, **2**:127-137.
50. MacConaill LE, Campbell CD, Kehoe SM, Bass AJ, Hatton C, Niu L, Davis M, Yao K, Hanna M, Mondal C, Luongo L, Emery CM, Baker AC, Philips J, Goff DJ, Fiorentino M, Rubin MA, Polyak K, Chan J, Wang Y, Fletcher JA, Santagata S, Corso G, Roviello F, Shivdasani R, Kieran MW, Ligon KL, Stiles CD, Hahn WC, Meyerson ML, *et al*: **Profiling critical cancer gene mutations in clinical tumor samples.** *PLoS One* 2009, **4**:e7887.
51. Romero PA, Arnold FH: **Exploring protein fitness landscapes by directed evolution.** *Nat Rev Mol Cell Biol* 2009, **10**:866-876.
52. Meylan E, Dooley AL, Feldser DM, Shen L, Turk E, Ouyang C, Jacks T: **Requirement for NF-kappaB signalling in a mouse model of lung adenocarcinoma.** *Nature* 2009, **462**:104-107.
53. Ding L, Ellis MJ, Li S, Larson DE, Chen K, Wallis JW, Harris CC, McLellan MD, Fulton RS, Fulton LL, Abbott RM, Hoog J, Dooling DJ, Koboldt DC, Schmidt H, Kalicki J, Zhang Q, Chen L, Lin L, Wendl MC, McMichael JF, Magrini VJ, Cook L, McGrath SD, Vickery TL, Appelbaum E, Deschryver K, Davies S, Guintoli T, Lin L, *et al*: **Genome remodelling in a basal-like breast cancer metastasis and xenograft.** *Nature* 2010, **464**:999-1005.
54. Shah SP, Morin RD, Khattra J, Prentice L, Pugh T, Burleigh A, Delaney A, Gelmon K, Guliany R, Senz J, Steidl C, Holt RA, Jones S, Sun M, Leung G, Moore R, Severson T, Taylor GA, Teschendorff AE, Tse K, Turashvili G, Varhol R, Warren RL, Watson P, Zhao Y, Caldas C, Huntsman D, Hirst M, Marra MA, Aparicio S: **Mutational evolution in a lobular breast tumour profiled at single nucleotide resolution.** *Nature* 2009, **461**:809-813.
55. Ellis IO, Schnitt SJ, Sastre-Garau X, *et al*: **Invasive breast carcinomas.** *Pathology and Genetics of Tumours of the Breast and Female Genital Organs* Lyon: IARC PressTavassoli FA, Devilee P 2003, 13-59.
56. Bibikova M, Talantov D, Chudin E, Yeakley JM, Chen J, Doucet D, Wickham E, Atkins D, Barker D, Chee M, Wang Y, Fan JB: **Quantitative gene expression profiling in formalin-fixed, paraffin-embedded tissues using universal bead arrays.** *Am J Pathol* 2004, **165**:1799-1807.
57. Fan JB, Yeakley JM, Bibikova M, Chudin E, Wickham E, Chen J, Doucet D, Rigault P, Zhang B, Shen R, McBride C, Li HR, Fu XD, Oliphant A, Barker DL,

Chee MS: **A versatile assay for high-throughput gene expression profiling on universal array matrices.** *Genome Res* 2004, **14**:878-885.
58. Da Silva L, Parry S, Reid L, Keith P, Waddell N, Kossai M, Clarke C, Lakhani SR, Simpson PT: **Aberrant expression of E-cadherin in lobular carcinomas of the breast.** *Am J Surg Pathol* 2008, **32**:773-783.
59. Kramer D, Thunnissen FB, Gallegos-Ruiz MI, Smit EF, Postmus PE, Meijer CJ, Snijders PJ, Heideman DA: **A fast, sensitive and accurate high resolution melting (HRM) technologybased assay to screen for common K-ras mutations.** *Cellular Oncology* 2009, **31**:161-167.

doi:10.1186/bcr2603
Cite this article as: Da Silva *et al.*: HER3 and downstream pathways are involved in colonization of brain metastases from breast cancer. *Breast Cancer Research* 2010 **12**:R46.

Additional file 1

Morphological review & TMA creation

Haematoxylin & eosin (H&E) sections were reviewed by three pathologists (LDS, MC, SRL) to confirm the diagnosis, assess morphology and grade the tumours according to the World Health Organization criteria[55]. Tissue microarrays (TMA) were built using the tissue arrayer, model MTAI (Beecher Instruments, Inc, Sun Prairie, WI 53590 USA) to facilitate screening of clinical samples using immunohistochemistry and in situ hybridization. H&E slides were dotted by LDS in order to take representative 0.6mm diameter cores of each tumour for analysis. Two cores were taken from each tumour. Two sets of TMAs were built. The first TMA set comprised 29 primary breast cancers and their matched brain metastases and 22 unmatched brain metastases. The second TMA set comprised 10 primary breast cancers and their matched brain metastases, as well as the 11 non-breast brain metastases. Slides and paraffin blocks from 38 tumor samples (primary breast cancer and metastases to multiple sites, including brain) from 8 autopsy cases of patients who died of metastatic breast cancer were also available.

Immunohistochemistry and chromogenic *in situ* hybridization

Four micron thick sections of the paraffin blocks were cut on to silane-coated slides. Immunohistochemistry was performed using the Envision® dual link system (Dakocytomation, Denmark) according to the manufacturer's recommendations. Supplementary table 1 summarises all antibody details. Antigenic retrieval for all antibodies (except smooth muscle actin (SMA) which did not require any antigen retrieval and EGFR – 5 minutes chymotrypsin digestion) required two minutes pressure cooking (105^{o}C) in EDTA (pH8.0) buffer. Positive and negative

controls were included in all runs and all slides were analysed by at least two pathologists (LDS, PP or SRL) using double headed optical light microscope. HER2 staining and scoring used a minimum 30% percent cut-off of positivity with strong complete membrane staining to regard a case as HER2 overexpressed (3+). The same criteria were used for EGFR, HER3 and HER4 and assessed in the periphery of the tumors. For all other antibodies, samples were considered positive if more than 10% of tumor cells were stained in one or both cores on the TMA. Cellular localization (membrane, cytoplasm, nuclear), staining intensity (negative, weak/1+, moderate/2+, strong/3+) and percentage/number of positively stained neoplastic cells was recorded. A tumor was regarded as 'basal' if any of the following markers were positive (CK5/6, CK14,CK17, p63, SMA, EGFR). The EGFR, HER3, HER4, CD44 and CD24 were assessed on whole sections and not as double stain. Digital slide images are available at http://aperio.qimr.edu.au/. The username is LeoExternal and password leoext1 (case sensitive) and the images are under the head "List all digital images". Chromogenic *in situ* hybridization was performed following instructions of the Zymed Spot-Light®HER2 CISH^{TM} Kit (Zymed, California, USA). Briefly, the paraffin embedded sections were dewaxed and subjected to heat and enzyme digestion treatments followed by denaturation and hybridization to labelled nucleic acid probes. Immunodetection was performed and 3, 3'-Diaminobenzidine tetrachloride was used for visualization. Slides were counterstained with haematoxylin. A positive control for HER2 amplification was included in each run. Signals were counted under a brightfield microscope and results were classified into diploid, polysomy, low amplification and high amplification according to the manufacture's recommendation. Immunohistochemistry using an antibody raised against the E746_A750del mutated EGFR protein was performed to validate Oncocarta® data. Myoepithelial cells of

normal breast tissue, which are normally positive for wild-type EGFR, were also used as negative control for the E746_A750del mutation antibody.

Supplementary Table 1 – Details of Antibodies Used in Immunohistochemistry

Antibody	Company	Clone – Dilution
ER	Novocastra	6F11 – 1:100
PR	Novocastra	1A6 – 1:500
HER2	DAKO	Herceptest®
HER3	Novus Biologicals	RTJ2 - 1:80
HER4	Santa Cruz	C-18 - 1:100
EGFR	Zymed	31G7 - 1:100
p63	DAKO	4A4 – 1:400
SMA	DAKO	1A4 – 1:100
p53	DAKO	D07- 1:100
CD44	DAKO	DF1485 – 1:100
CD24	Serotec	SN3 – 1:200
CK5/6	DAKO	D5/16B4 – 1:50
CK14	Neomarkers	LL002 – 1:50
E-cadherin	Zymed	HECD-1 1:20
CK19	DAKO	RCK108 – 1:25
CK7	DAKO	OV-TL12/30 – 1:500
CK17	DAKO	E3 -1:100
CK8/18	Novocastra	5D3- 1:100
Phospho HER3	Cell Signalling	Tyr^{1289}(21D3) -1:300
Phospho AKT	Invitrogen	pT^{308}-1:300
Phospho ERK1/ERK2	Invitrogen	pTpY $^{185/187}$-1:300
Phospho JNK1/2	Invitrogen	pTpY $^{183/185}$-1:300
Phospho ERK5	Invitrogen	pTpY $^{180/182}$-1:300
p38	Invitrogen	pTpY $^{218/220}$-1:300
Mutated-EGFR	Cell Signalling	E746-A750del(6b6) – 1:100
Ki-67	Dako	MIB1 -1:100
GRB2	Cell Signalling	1:100
HIF1-alfa	Cell Signalling	1:100

RNA extraction and Real-Time RT-PCR

Three 5μm thick FFPE sections of clinical samples were cut and de-waxed in two lots of xylene and two lots of 100% ethanol, 10 minutes each. RNA was extracted using the High Pure RNA

Paraffin Kit® (Roche Applied Science, Mannheim, Germany) according to the manufacturer's protocol. RNA was quantified using the NanoDrop® ND-1000 (NanoDrop Technologies, DE, USA). Relative expression levels of *HER3, HER2, EGFR, HER4, HIF1-alfa and CCNH* was assessed using RT-PCR. Complementary DNA (cDNA) was synthesized from 240ng of total RNA using random hexamers and the SuperScript^{TM} III Reverse Transcriptase kit (Invitrogen, Carsbald, CA, USA). TaqMan One-Step UniversalMaster Mix (Applied Biosystems) was used for all reactions. TaqMan reaction was done in a standard 96-well plate format with ABI 7500 OneStepPlus PCR system. For data analysis, raw deltaCt (dCt) was first normalized to an endogenous control gene (RPL13a) for each sample to generate normalized dCt. The normalized dCt was then calibrated to a cell line pool reference (MCF-7, SKBR-3 and MDA-MB-231) to generate a ddCt. In the final step of data analysis, the ddCt was converted to fold change (2^{-ddCt}) relative to the reference allowing comparison between samples.

DASL gene expression profiling

Gene expression profiling was performed using the DASL assay (cDNA-mediated annealing, selection extension and ligation, Illumina Inc., California, USA) to interrogate the DASL Cancer Panel that contained 512 cancer related genes [56-58]. All protocols were as specified by Illumina Inc. Briefly, RNA (250ng) was converted to cDNA through a reverse transcription reaction with biotinylated oligo-d$(T)_{18}$ and random nonamers. Gene specific oligonucleotides (three unique pairs for each of the 512 genes) were annealed to the biotinylated cDNA, the duplexes were bound to streptavidin conjugated paramagnetic particles to remove non-hybridized oligos. The annealed oligos were then extended and ligated (to incorporate an address sequence and primer site) to generate amplifiable products. These products were subjected to

PCR amplification using fluorescently labeled (Cy3 and Cy5) primers. The labeled PCR products were hybridized to a Sentrix array or Beadchip. Following hybridization, the arrays were scanned with a BeadArray Reader (Illumina) and data was extracted using BeadStudio version 3 software (Illumina). Samples exhibiting a median hybridization intensity across all probes of <600 (background corrected) were excluded from analysis. Individual probes with a BeadStudio detection score greater than 0.99 in more than 15 conditions were included which left 1234 probes in the analysis. Array data transformation and normalization (per chip normalized to 50th percentile and per gene normalized to median) was done in Genespring® version 7.0 software (Agilent Technologies, Santa Clara, USA). Hierarchical clustering was performed using Pearson Correlation and Average Linkage clustering algorithm. Principal component analysis was also performed. A linear model was fitted (limma) and a moderated t-statistic was performed for differential expression. DASL data is available from Gene Expression Omnibus (http://www.ncbi.nlm.nih.gov/geo/, Accession number GSE14690).

Cell lines

SUM159 and BT20 mammospheres were grown in 5 ml of serum-free DMEM/F12 (NSA) medium containing freshly added 20 ng/ml rhEGF (R&D Systems), 10 ng/ml rhFGF (R&D Systems), 4 ug/ml heparin, 10% proliferation supplement (NeuroCult®, Stem Cell Technologies Inc.), 2% BSA (Sigma). Breast cancer cell lines MCF-7, MDA-MB-231 and SKBR-3 were cultured in Dulbecco's Modified Eagle's Medium (DMEM) plus 10% heat-inactivated fetal bovine serum (FBS), 2 mmol/L glutamine, and 1% penicillin G-streptomycin solution.

OncoCarta somatic mutation analysis

Oncogenic mutations in tumour samples were profiled using the OncoCarta Assay Panel v1.0, which offers rapid, parallel analysis of 238 mutations across 19 common oncogenes. All reactions were performed according to the OncoCarta v1.0 User's Guide (Sequenom, San Diego, CA). PCR amplification was carried out using 20 ng DNA as a template for each Assay. Post-PCR treatment by shrimp alkaline phosphatase was followed by the TypePLEX Extend Reaction. Following this step, CLEAN Resin (Sequenom) was added to the mixture to remove extraneous salts that could interfere with the MALDI-TOF analysis. Allelotyping was determined by robotically spotting 15 nl of each extension product onto a SpectroCHIP II, which was subsequently read by the MassARRAY Compact Analyzer. Some mutations were validated with a second OncoCarta analysis, using just a subset of primers that detect the relevant *EGFR* mutations. Poor quality samples were identified by evaluating the primer extension rates. All samples in which more than 10% of assays had less than 50% primer extension were defined as 'poor quality' and removed from further analysis.

High Resolution Melt Analysis

For cases with sufficient DNA available, we carried out High Resolution Melt (HRM) analysis to validate mutations in *KRAS, HRAS, NRAS* and *PIK3CA* identified with the OncoCarta Assay. Primers used for HRM Analysis were the same as those used in the OncoCarta Assay Panel and are shown in Supplementary Table 2. PCR reactions for HRM for *KRAS, HRAS, NRAS* and *PIK3CA* were performed on a LightCycler 480 (Roche Diagnostics, Mannheim, Germany) in 10ul final volume containing 1x LightCycler 480 High Resolution Melting Master Mix (Roche Diagnostics), 500 nM forward primer, 500 nM reverse primer, 30 mM $MgCl_2$ and 10 ng genomic DNA. The cycling conditions were as follows: Pre-incubation at 95°C for 5min, followed by 26

cycles of 95°C for 10 s, touchdown from 65°C to 53°C (-0.5°C/cycle) for 10 s and 72°C for 10 s, followed by a further 19 cycles at 53°C annealing temperature. The melting program consisted of one cycle at 95°C for 1 min, 40°C for 1 min and then continuous fluorescent reading from 65 to 95°C at 25 acquisitions per °C. HRM data were analysed using the LightCycler 480 Gene Scanning Software (Roche Diagnostics) as previously described [59].

Supplementary Table 2 - Primers used for HRM Analysis

Primer name	Targeted Mutation	Primer Sequence	Product Size
NRAS_6 - 1st Primer	Q61R	ACGTTGGATGTCGCCTGTCCTCATGTATTG	99
NRAS_6 - 2nd Primer		ACGTTGGATGCCTGTTTGTTGGACATACTG	
PIK3CA_6 - 1st Primer	E545K	ACGTTGGATGTACACGAGATCCTCTCTCTG	90
PIK3CA_6 - 2nd Primer		ACGTTGGATGTAGCACTTACCTGTGACTCC	

Sequencing

For cases with sufficient DNA available, and an OncoCarta Assay result of ≥ 30% mutant allele proportion (MAP) for *KRAS, HRAS, NRAS* and *PIK3CA* we used direct sequencing for validation. Primers for sequencing (Supplementary Table 3) were designed using the web-based programme Primer 3 (http://frodo.wi.mit.edu/primer3/). PCR reactions were performed in a final volume of 20 µl and contained 15 ng DNA, 200 nM of each primer, 250 µM dNTPs, 1× PCR buffer with 2 mM $MgCl_2$, and 1 U i-STAR Taq polymerase (Scientifix, Clayton, Australia). Touchdown amplification was as follows : 94°C for 12 min, followed by four sets of four cycles of 94°C for 30 s, 61°C to 55°C for 45 s and 72°C for 30 s, with the annealing temperature dropping 2°C after each set of four cycles, followed by 30 cycles of 94°C for 30 s, 55°C for 45 s and 72°C for 30 s, and a final extension of 72°C for 7 min. PCR reactions were purified with the QIAGEN PCR purification kit and sequenced using Big-Dye (version 3.1) sequencing chemistry

and the PE Applied Biosystems 377 sequencer. The resulting chromatograms were compared with wild type samples which were sequenced as controls.

Supplementary Table 3 - Primers for sequencing

Primer name	Targeted Mutation	Primer Sequence	Product Size
KRAS1-2/4_(G12C/G13D)-F	G12C and G13D	TTAACCTTATGTGTGACATGTTCTAA	171
KRAS1-2/4_(G12C/G13D)-R		TGGATCATATTCGTCCACAAAA	
NRAS2_(G12C)-F	G12C	GATGTGGCTCGCCAATTAAC	175
NRAS2_(G12C)-R		CTCACCTCTATGGTGGGATCA	
NRAS6_(Q61R)-F	Q61R	CACCCCCAGGATTCTTACAG	173
NRAS6_(Q61R)-R		TCCGCAAATGACTTGCTATT	
PIK3CA9_(H1047L)-F	H1047L	TGAGCAAGAGGCTTTGGAGT	190
PIK3CA9_(H1047L)-R		GGTCTTTGCCTGCTGAGAGT	

iPLEX genotpying

For cases with sufficient DNA available, we used Sequenom's MassARRAY system and iPLEX technology to validate mutations in *NRAS, PIK3CA* and *EGFR* identified with the OncoCarta Assay. The design of oligonucleotides was carried out according to the guidelines of Sequenom Inc. and performed using MassARRAY Assay Design software (version 1.0). Four-Plex PCR amplification of amplicons containing variants of interest was performed using Qiagen HotStart Taq Polymerase on a Perkin Elmer GeneAmp 2400 thermal cycler with 5 ng genomic DNA in a 2.5 μl reaction. Primer extension reactions were carried out according to manufacturer's instructions for iPLEX chemistry. Assay data were analysed using Sequenom TYPER software (Version 3.4).

Supplementary Table 4 - Primers for iPLEX

Primer name	Mutation	Primer Sequence	Product Size
NRAS_Q61R_q1	Q61R	ACGTTGGATGCCTGTTTGTTGGACATACTG	
NRAS_Q61R_q2		ACGTTGGATGTCGCCTGTCCTCATGTATTG	
NRAS_Q61R_q3		TGGCACTGTACTCTTCT	
PIK3CA_E545K_q1	E545K	ACGTTGGATGTACACGAGATCCTCTCTCTG	
PIK3CA_E545K_q2		ACGTTGGATGTAGCACTTACCTGTGACTCC	
PIK3CA_E545K_q3		AGAAAATCTTTCTCCTGCT	
PIK3CA_H1047R_iPlex-F	H1047R	ACGTTGGATGAACTGAGCAAGAGGCTTTGG	
PIK3CA_H1047R_iPlex-R		ACGTTGGATGTCCATTTTTGTTGTCCAGCC	
PIK3CA_H1047R_iPlex-Ext		ATGAAACAAATGAATGATGCAC	
HRAS_G13S_iPlex-F	G13S	ACGTTGGATGAATGGTTCTGGATCAGCTGG	
HRAS_G13S_iPlex-R		ACGTTGGATGGACGGAATATAAGCTGGTGG	
HRAS_G13S_iPlex-Ext		CGCACTCTTGCCCACAC	
NRAS_G12C_iPlex-F	G12C	ACGTTGGATGAGTGGTTCTGGATTAGCTGG	
NRAS_G12C_iPlex-R		ACGTTGGATGGACTGAGTACAAACTGGTGG	
NRAS_G12C_iPlex-Ext		GCTTTTCCCAACACCAC	
EGFR_E746_A750del_iPlex-F	E746_A750del	ACGTTGGATGGATCCCAGAAGGTGAGAAAG	
EGFR_E746_A750del_iPlex-R		ACGTTGGATGTCGAGGATTTCCTTGTTGGC	
EGFR_E746_A750del_iPlex-Ext		AATTCCCGTCGCTATCAA	
PIK3CA_R38H_iPlex-F	R38H	ACGTTGGATGGGGGTATTTTCTTGCTTCTT	
PIK3CA_R38H_iPlex-R		ACGTTGGATGCCAAATGGAATGATAGTGAC	
PIK3CA_R38H_iPlex-Ext		ATGGTTATTAATGTAGCCTCA	

Additional file 2

Table 1 – Immunohistochemistry results

Antibody	Primary breast tumor N/T (%)	Matched brain metastases N/T (%)	Unmatched brain metastases N/T (%)	Non-breast brain metastases N/T (%)
ER	15/37(40%)	15/37 (40%)	4/21 (23%)	NP
PR	9/37 (24%)	9/37 (24%)	5/21 (19%)	NP
HER2	7/34 (20%)	7/35 (19%)	5/24 (20%)	NP
Triple negative	19/29(56%)	20/35(48%)	10/22(45%)	NP
CK5/6	9/26 (34%)	9/26 (34%)	2/16 (12%)	NP
CK14	15/35 (42%)	16/36 (44%)	8/16 (50%)	NP
CK17	5/26 (19%)	5/26 (19%)	5/16 (30%)	NP
EGFR	6/26 (23%)	6/26 (23%)	3/16 (18%)	9/11 (81%)
p63	0/26	0/26	1/15 (5%)	NP
SMA	6/26 (23%)	6/26 (23%)	2/15 (13%)	NP
Basal-like	20/37 (54%)	21/35 (60%)	11/22 (50%)	NP
CD44	5/20 (25%)	13/20 (65%)	10/22 (45%)	NP
CD24	5/22 (22%)	2/22 (9%)	3/22 (14%)	NP
$CD44^{+}CD24^{-}$	5/20(25%)	11/20 (55%)	10/22(45%)	NP
p53	16/26 (61%)	19/26 (73%)	14/20 (70%)	NP
KI-67	19/37(51%)	32/37 (86%)	18/21 (85%)	NP
CK19	24/26 (92%)	24/26 (92%)	15/15 (100%)	NP
CK8/18	14/26 (53%)	14/26 (53%)	15/15 (100%)	NP
E-cadherin	19/26 (73%)	19/23 (82%)	18/18 (100%)	NP
HER3	11/37 (29.7%)	22/37 (59%)	13/21 (62%)	NP
HER4	7/35(20%)	6/26 (23%)	5/24 (20%)	NP
Phospho HER3	14/37 (38%)	24/37 (64%)	18/21 (85%)	0/11
Phospho AKT	32/37 (86%)	32/37 (86%)	15/21 (71%)	11/11 (100%)
Phospho ERK1/2	28/37 (75%)	36/37 (97%)	20/21(95%)	11/11 (100%)
Phospho JNK1/2	26/37 (70%)	34/37 (91%)	19/21 (90%)	11/11 (100%)
Phospho ERK5	29/37 (78%)	36/37 (97%)	20/21 (95%)	11/11 (100%)
p38	29/37(78%)	37/37 (100%)	21/21 (100%)	11/11(100%)
GRB2	13/36 (36%)	16/36 (44%)	11/22 (50%)	NP
HIF1-alfa	9/37 (24%)	20/35(48%)	8/16 (50%)	NP

Legend: N = number of tumor cases showing positivity; T = total number of cases assessable for the antibody specified; % = percentage of cases showing positivity; NP = not performed; A tumor was regarded as 'basal' if any of the following markers were positive (CK5/6, CK14, CK17, p63, SMA, EGFR,) in more than 10% of cells. Triple negative tumors were negative for ER, PR and HER2. CD44+/CD24- immunohistochemistry was assessed on serial sections and positivity was expression in >10% cells. X^2 test with Yates correction (95% confidence interval) showed significant differences between matched primaries and metastases as follow: phospho-Her3 p =0.046, phosphor-ERK1/2 p= 0.017, phosphor-ERK5 p=0.032, phosphor-JNK p= 0.037, p38 p=0.008, HER3 p=0.019, HIF1-alfa p=0.009 and CD44 p=0.026. GRB2 showed a trend p=0.1

Figure 1 - Scatter plots showing distribution of positivity for ER, phospho-HER3, phospho-ERK1/2 and phospho-ERK5 across matched and unmatched samples. Panel on left shows the correlation of immunohistochemical score between primary tumor (x-axis) and the matched metastasis (y-axis). The panel on the right shows the immunohistochemical score (y-axis) for each marker in individual unmatched metastases (x-axis).

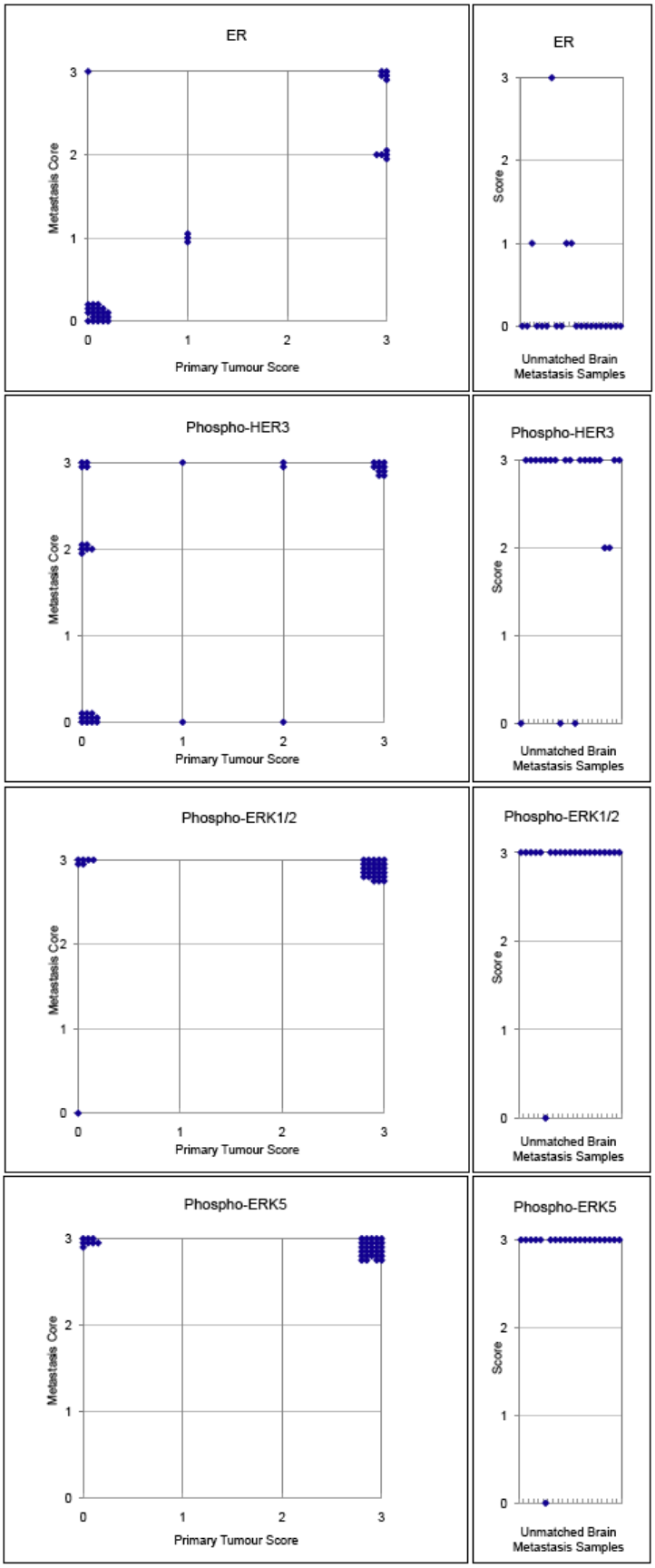

Figure 2: Principal component analysis using the 27 gene list from figure 2B showing good separation between brain metastases (red squares) and primaries (blue squares).

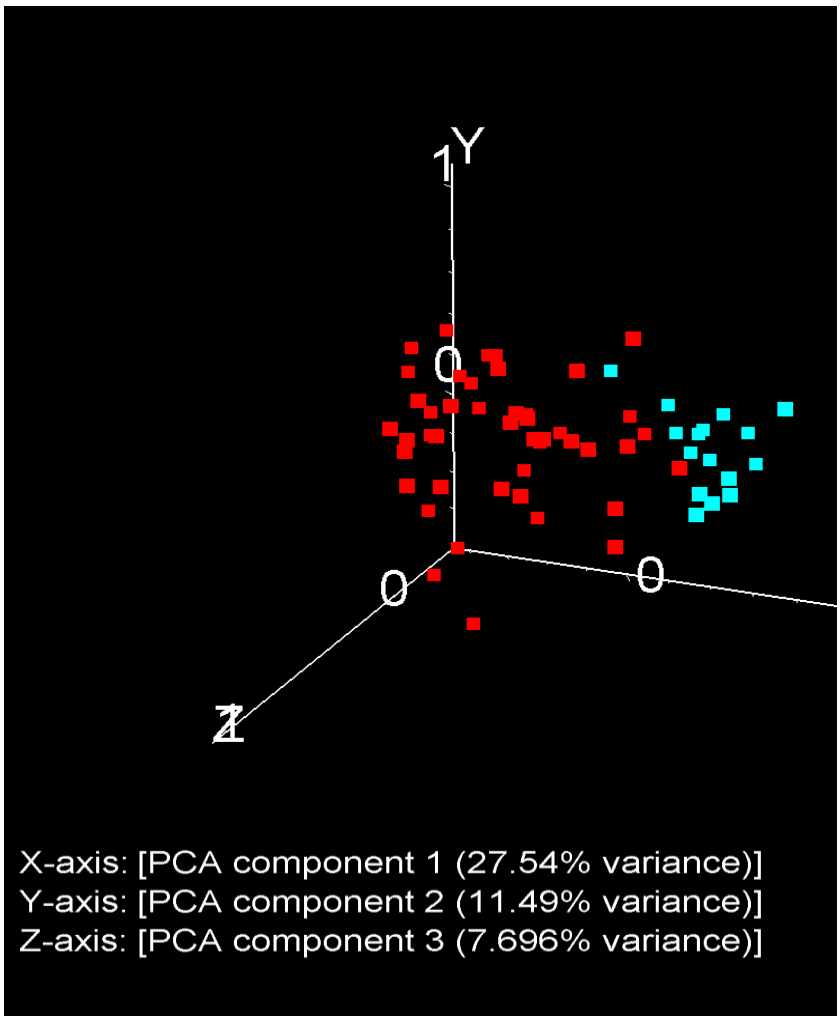

Table 2: Somatic mutations in autopsy samples

Case ID#	Site	GRADE	*EGFR*		*PIK3CA*	
			Mutation	MAP	Mutation	MAP
1	Breast	3				
	Brain					
	Lung					
	Mediastinal lymph node					
	Adrenal gland					
2	Brain				H1047R[I, S]	57.6%
	Liver				H1047R[I,Y]	54.9%
	Breast	3			H1047R[I,Y]	54.7%
	Peritoneum				H1047R[I,Y]	65.0%
	Lung				H1047R[I,Y]	53.1%
5	Axillary lymph node					
	Breast	3				
	Adrenal gland					
	Lung					
6	Ovary					
	Brain					
	Brain					
	Breast	2				
7	Liver		E746_A750del[O, I,A]	12.7%	R38H[X, Y]	20.7%
	Brain					
	Axillary lymph node					
8	Lymph node		H773_V774insNPH[NVP]	27.4%		
	Pituitary/hypothalamus					
	Pleura					
	Breast					
	Pancreas					

MAP = Mutant Allele Proportion estimated by OncoCarta
NVP = no validation possible because no DNA remained
O = validated by repeat OncoCarta analysis using a subset of assays that included primers for EGFR G719S, D770_N771insG, and E746_A750del mutations
S = validated by sequencing
A = validated by immunohistochemistry using a mutation-specific antibody
I = validated by iPLEX using diferent primers from the OncoCarta assay
X = iPLEX didn't work for this sample
Y = Sequencing did not work for this sample

Figure 3: RT-PCR and DASL assay for HER receptors genes and HIF1-alfa summary

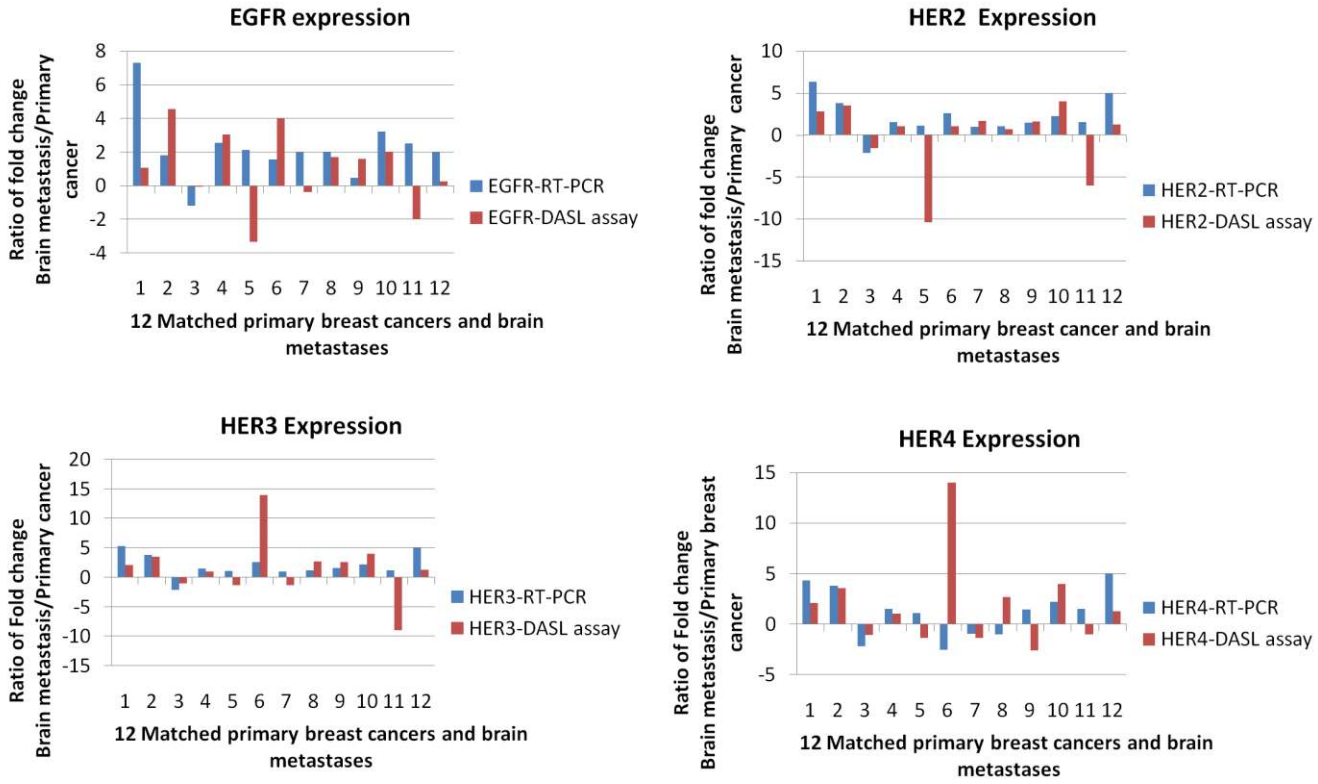

Summary of RT-PCR and DASL assay for 12 matched samples – Positive values indicate increased fold change in metastases and negative values increased fold change in primary cancers

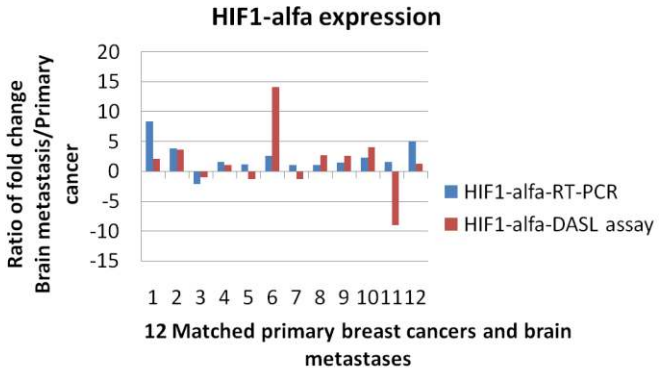

Summary of RT-PCR and DASL assay for 12 matched samples – Positive values indicate increased fold change in metastases and negative values increased fold change in primary cancers